RESEARCH ARTICLE | JULY 02 2025

Millimeter Wave Spectrum and Rovibrational Global Fit for Pyrrole

A. Maris ; L. Evangelisti ; S. Melandri

J. Phys. Chem. Ref. Data 54, 033101 (2025)
https://doi.org/10.1063/5.0278157

Journal of Physical and Chemical Reference Data ARTICLE pubs.aip.org/aip/jpr

Millimeter Wave Spectrum and Rovibrational Global Fit for Pyrrole

Cite as: J. Phys. Chem. Ref. Data 54, 033101 (2025); doi: 10.1063/5.0278157
Submitted: 28 April 2025 • Accepted: 2 June 2025 •
Published Online: 2 July 2025

A. Maris,[a] L. Evangelisti, and S. Melandri

AFFILIATIONS

Department of Chemistry G. Ciamician, University of Bologna, Bologna I-40129, Italy

[a]**Author to whom correspondence should be addressed:** assimo.maris@unibo.it. **URL:** https://site.unibo.it/freejet/en.
Also at: Interdepartmental Center for Industrial Aerospace Research (CIRI Aerospace), University of Bologna, Forlì I-47121, Italy.

ABSTRACT

The free-jet millimeter wave absorption spectrum of pyrrole has been measured in the 59.6–78.3 GHz frequency range. The rotational spectra of four species have been assigned: the one for the normal species in both the vibrational ground state and the first excited state of the NH out-of-plane bending and those of two ^{13}C monosubstituted isotopologues observed in natural abundance. For each species, the hyperfine structure due to the nuclear quadrupole coupling interaction of the ^{14}N nucleus with the overall rotation has been resolved. The new rotational data for the ground state and the vibrational satellite were analyzed simultaneously with existing microwave/millimeter-wave data and rovibrational data for the fundamental [$\tilde{\nu}$ = 474.647 552(5) cm^{-1}], first overtone [$\tilde{\nu}$ = 962.720 890(5) cm^{-1}], and first hot bands of the NH out-of-plane bending motion. A comprehensive list of lines and the resulting set of spectroscopic parameters are provided.

CONTENTS

List of Tables

List of Figures

1. Introduction

Pyrrole, also known as azacyclopentadiene (c–C_4H_4NH), is a five-membered heterocyclic aromatic ring with C_{2v} symmetry. Although it is not naturally occurring, pyrrole serves as the building block for tetrapyrrole, porphyrin, and corrin macrocycles, which form the active cores of essential biomolecules such as chlorophyll, heme, cobalamin, and cofactor F430. Laboratory experiments simulating the interaction of molten lava with seawater containing amino acids led Fox and Strasdeit[1] to suggest that pyrrole and some of its oligomers could be abiotically synthesized on primordial volcanic islands, potentially making them available to the first protocells.

The rotational spectrum of pyrrole has been extensively studied over four decades, from the 1950s to the 1980s. The first assignment in the microwave region was conducted by Wilcox and Goldstein[2] in 1952, followed by the Bak *et al.*[3] study on the normal and deuterated forms in 1956. In 1969, Nygaard *et al.*[4] resolved the hyperfine structure due to ^{14}N nuclear quadrupole coupling and assigned the spectra of the ^{13}C and ^{15}N isotopologues. Further insights into the hyperfine structure were provided by two independent studies in 1974 by Bolton and Brown[5] and Gaines *et al.*,[6] and later by Bohn, Hillig, and Kuczkowski[7] in 1989. Notably, using a maser spectrometer, Gaines *et al.*[6] also disentangled the spin-spin interaction effect and determined the spin-rotation tensor elements (three for each type of proton and nitrogen). Finally, measurements in the millimeter spectral region up to 260 GHz in 1988 by Wlodarczak *et al.*[8] allowed for a precise determination of the centrifugal distortion constants. The main spectral features of these experiments are summarized in Table 1. A global fit for the normal species, including both microwave[4,5] and millimeter wave[8] measurements, but omitting the ^{14}N hyperfine structure, was provided by Wlodarczak *et al.*[8] and later re-proposed by Müller at the Cologne Database for Molecular Spectroscopy (CDMS),[9] where the input and output files are available (https://cdms.astro.uni-koeln.de/cdms/portal/catalog/1297/#).

Further information comes from high-resolution infrared studies, where pyrrole spectra have been disentangled through vibro-rotational analysis. Following the pioneering study on the fundamental NH stretching band (1_0^1) by Eloranta[10] in 1970, thirteen fundamental bands,[11–16] one hot band,[14,15] and three overtone bands[12,17] have been investigated, as detailed in Table 2.

Regarding the simultaneous fit of pure rotational and rovibrational transition lines, to our knowledge, only the work of Mellouki, Auwera, and Herman[13] is available, where the rotational data of Wlodarczak *et al.*[8] were used alongside data related to the funda-

TABLE 2. Rotationally resolved vibrational bands of pyrrole. The normal modes are classified according to their symmetry representation Γ as defined by Bunker and Jensen,[28] and the numbering corresponds to the Mulliken[29] convention

$v_v^{v'}$	Γ	Selection rule	$\tilde{\nu}_0$ (cm^{-1})
1_0^1	a_1	*a*-type	3530.811[11]
1_0^2	a_1	*a*-type	6924.630[12]
1_0^3	a_1	*a*-type	10 184.174[17]
3_0^1	a_1	*a*-type	3127.872[12]
7_0^1	a_1	*a*-type	1074.623[14]
8_0^1	a_1	*a*-type	1016.945[14]
9_0^1	a_1	*a*-type	881.130[16]
13_0^1	b_1	*c*-type	826.893[16]
14_0^1	b_1	*c*-type	722.133[13]
16_0^1	b_1	*c*-type	474.648[15]
16_1^2	b_1	*c*-type	488.1[15]
16_0^2	a_1	*a*-type	962.721[14,15]
17_0^1	b_2	*b*-type	3143.157[12]
18_0^1	b_2	*b*-type	3118.301[12]
20_0^1	b_2	*b*-type	1424.378[14]
23_0^1	b_2	*b*-type	1049.120[14]
24_0^1	b_2	*b*-type	865.443[16]

TABLE 1. Survey of the rotational spectroscopy investigations on pyrrole

Range (GHz)	Accuracy (MHz)	*hfs*[a]	Isotopologues	Vib. state[b]	Reference
1–5	0.001	Yes	⋯	GS	Gaines *et al.*[6]
4–14	0.010	Yes	⋯	GS	Bolton and Brown[5]
12–15	0.005	Yes	⋯	GS	Bohn, Hillig, and Kuczkowski[7]
12–25	0.100	Yes	2-^{13}C, 3-^{13}C, ^{15}N, 1-^{2}H, 2-^{2}H, 3-^{2}H	GS	Nygaard *et al.*[4]
17–26	0.100	No	1-^{2}H, 2-^{2}H, 3-^{2}H, 2, 3, 4, 5-^{2}H, 1, 2, 3, 4, 5-^{2}H	GS	Bak *et al.*[3]
22–32	1.000	No	⋯	GS	Wilcox and Goldstein[2]
67–78	0.050	Yes	2-^{13}C, 3-^{13}C	GS, $v(\nu_{16}) = 1$	This work
149–260	0.050	No	⋯	GS	Wlodarczak *et al.*[8]

[a]The *hfs* column indicates whether the hyperfine structure resulting from the nuclear quadrupole coupling interaction was observed.
[b]GS indicates the vibrational ground state.

mental bands of both the symmetric out-of-plane CH bending (14_0^1) and NH stretching (1_0^1).[13] The authors determined the rotational constants, quartic centrifugal distortion constants, and some sextic components using Watson's S-reduction and both the I^r and III^r representations for the ground state and the fundamentals. The determined ground state spectroscopic constants were used as reference data by subsequent rovibrational studies. However, the specific line list used by Mellouki, Vander Auwera, and Herman[13] is not available, preventing a direct refinement of their model. Therefore, building upon newly available high-resolution literature data on the NH out-of-plane bending vibrational bands (16_0^1, 16_0^2 and 16_1^2)[14,15] and new rotational spectroscopy measurements presented here, we propose an alternative global fit that explicitly includes the ^{14}N nuclear quadrupole coupling, aiming to provide a comprehensive and critically evaluated set of spectroscopic parameters for pyrrole and its isotopologues. These results are useful for characterising pyrrole by spectroscopic methods and provide a complete set of high-resolution data that can aid its detection in astronomical surveys.

2. Experimental Methods

Pyrrole (purity 99%, *b.p.* 404 K, *m.p.* 250 K) was purchased from Merck and used without further purification. It was analyzed in the 59.6–78.3 GHz frequency region using a Stark-modulated free-jet absorption millimeter-wave (FJ-AMMW) spectrometer, previously described.[18,19] A gas mixture of pyrrole and argon was prepared by flowing 300 kPa of argon over a sample of liquid pyrrole maintained at room temperature (*v.p.* 1.1–1.4 kPa). Using a stagnation pressure of P_0 = 20 kPa, the gas mixture was expanded into a vacuum chamber through a pinhole nozzle with a diameter of 0.35 mm. This setup allowed for the recording of the rotational spectrum under supersonic jet expansion conditions, with an estimated rotational temperature of ~10 K.[20,21] The estimated accuracy of the frequency measurements is about 50 kHz, allowing the resolution of lines separated by more than 300 kHz.

3. Symmetry Properties

Pyrrole is a planar molecule belonging to the C_{2v} symmetry point group (see Fig. 1). The C_2 symmetry axis corresponds to the *a*-principal axis, and the molecule lies on the *ab* inertial plane. The permanent electric dipole moment is μ = 1.767(2) D and lies along the *a*-axis.[7] Consequently, the pure rotational spectrum consists of *a*-type transitions, which involve levels with K_a values of the same parity. The transition intensities reflect the presence of two pairs of equivalent fermions, resulting in a statistical nuclear spin-weight ratio of 5:3 for *ortho*-pyrrole to *para*-pyrrole. In the vibrational ground state, the *ortho* states are characterized by even K_a values, while the *para* states have odd K_a values. According to Mellouki, Liévin, and Herman,[22] pyrrole has 24 vibrational normal modes with the following symmetry representation:

$$\Gamma = 9 \cdot a_1 + 3 \cdot a_2 + 4 \cdot b_1 + 8 \cdot b_2 \quad (1)$$

The a_2 fundamentals are infrared inactive, while the a_1, b_2, and b_1 fundamental bands are governed by *a*, *b*, and *c*-type selection rules, respectively.

4. Results

The spectrum of pyrrole recorded by a FJ-AMMW spectrometer reveals four series of transition lines showing a nuclear hyperfine structure at about 68 and 77 GHz, as detailed in Table 3. The most intense transition lines correspond to the vibrational ground state of the normal species. Weak features are assigned to the two ^{13}C monosubstituted species with 0.2% natural abundance due to the C_{2v} molecular symmetry. Intermediate intensity transition lines are associated with the first excited vibrational state of the out-of-plane bending motion of the NH group (ν_{16}). This mode, the lowest frequency normal mode of pyrrole, has a fundamental of 474.647 533(9) cm^{-1} as determined by Tokaryk and van Wijngaarden[15] through a simultaneous fit of three rotationally-resolved bands involving the ν_{16}: the fundamental band (16_0^1), the first overtone (16_0^2) and the first hot band (16_1^2), while the spectroscopic parameters of the ground state were fixed to those established by Mellouki, Vander Auwera, and Herman.[13]

4.1. Normal species

The rotational energy levels of the top asymmetric molecules are identified by the quantum number *J* and the pseudo-quantum numbers K_a and K_c, typically written as J_{K_a,K_c} or $J(K_a,K_c)$.[23] *J* quantifies the total rotational angular momentum of the entire molecule. K_a and K_c represent the total rotational angular momentum projections onto the *a* and *c* inertial axes, respectively.

Twenty-two μ_a-type rotational transition lines with lower values *J* ranging from 2 to 9 were identified for the normal species of pyrrole (Table 3). Six pairs of lines exhibit K_a-asymmetry degeneracy, with two pairs belonging to the *Q* branch and the remaining pairs to the *R* branch.

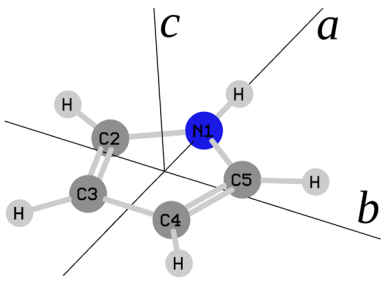

C_{2v}	E	$C_2(a)$	$\sigma_v(ac)$	$\sigma_v(ab)$
A_1	1	1	1	1
A_2	1	1	−1	−1
B_1	1	−1	1	−1
B_2	1	−1	−1	1

FIG. 1. Left: Sketch of pyrrole and its principal axis system. Right: Character table of the C_{2v} symmetry point group.

TABLE 3. Rotational transition lines of pyrrole: Newly measured frequencies (in MHz) are provided for the ground state ($v = 0$) and the first vibrational excited state ($v = 1$, NH out-of-plane bending mode) of the normal species and its ^{13}C isotopologues. Observed minus calculated (o.-c., in MHz) values, derived from global fittings, are also listed

J'	K_a'	K_c'	F'	J''	K_a''	K_c''	F''	$v = 0$	o.-c.	$v = 1$	o.-c.	2-^{13}C	o.-c.	3-^{13}C	o.-c.
4	3	1	4	3	3	0	4	67 339.92	0.01	67 259.55	0.00				
4	3	1	3	3	3	0	2	67 340.69[a]	0.14	67 260.35[a]	0.16	66 525.91[a]	0.09	65 618.02[a]	0.12
4	3	1	5	3	3	0	4	67 340.69[a]	0.02	67 260.35[a]	0.05	66 525.91[a]	−0.02	65 618.02[a]	0.01
4	3	1	4	3	3	0	3	67 340.69[a]	−0.12	67 260.35[a]	−0.07	66 525.91[a]	−0.14	65 618.02[a]	−0.11
4	3	1	3	3	3	0	3	67 341.75	−0.02	67 261.38	0.02				
3	2	1	3	2	0	2	2	67 612.87	0.01	67 485.82	0.00				
3	2	1	3	2	0	2	3	67 613.73[a]	0.00	67 486.62[a]	−0.04				
3	2	1	2	2	0	2	2	67 613.73[a]	−0.01	67 486.62[a]	−0.08				
3	2	1	4	2	0	2	3	67 614.40	0.02	67 487.32	0.01				
3	2	1	2	2	0	2	1	67 615.10	0.01	67 488.00	0.00				
5	3	3	4	4	3	2	3	67 971.33[a]	0.03	67 887.11[a]	0.07	67 155.80[a]	0.07	67 028.96[a]	0.01
5	3	3	6	4	3	2	5	67 971.33[a]	−0.04	67 887.11[a]	0.00	67 155.80[a]	−0.01	67 028.96[a]	−0.07
5	3	3	5	4	3	2	4	67 971.65	0.00	67 887.41	0.03	67 156.10	0.02	67 029.28	−0.02
5	2	3	4	4	3	2	3					67 154.74[a]	0.07	67 016.29[a]	0.02
5	2	3	6	4	3	2	5					67 154.74[a]	−0.01	67 016.29[a]	−0.06
5	2	3	5	4	3	2	4					67 155.03	0.01	67 016.67	0.05
7	0	7	6	6	0	6	6	67 980.72[a]	0.01	67 956.80[a]	0.03				
7	1	7	6	6	1	6	6	67 980.72[a]	0.01	67 956.80[a]	0.03				
7	0	7	8	6	0	6	7	67 982.46[a]	0.04	67 958.48[a]	0.06	67 167.05[a]	0.05	67 105.94[a]	0.04
7	1	7	8	6	1	6	7	67 982.46[a]	0.04	67 958.48[a]	0.06	67 167.05[a]	0.05	67 105.94[a]	0.04
7	0	7	6	6	0	6	5	67 982.46[a]	0.01	67 958.48[a]	0.04	67 167.05[a]	0.02	67 105.94[a]	0.01
7	1	7	6	6	1	6	5	67 982.46[a]	0.01	67 958.48[a]	0.04	67 167.05[a]	0.02	67 105.94[a]	0.01
7	0	7	7	6	0	6	6	67 982.46[a]	−0.03	67 958.48[a]	0.00	67 167.05[a]	−0.02	67 105.94[a]	−0.02
7	1	7	7	6	1	6	6	67 982.46[a]	−0.03	67 958.48[a]	0.00	67 167.05[a]	−0.02	67 105.94[a]	−0.02
6	2	5	5	5	2	4	5	67 984.41[a]	0.00	67 929.47[a]	0.03				
6	1	5	5	5	1	4	5	67 984.41[a]	0.00	67 929.47[a]	0.02				
6	2	5	5	5	2	4	4	67 985.08[a]	0.00	67 930.13[a]	0.04	67 169.69[a]	0.05	67 109.35[a]	0.12
6	1	5	5	5	1	4	4	67 985.08[a]	−0.01	67 930.13[a]	0.03	67 169.69[a]	0.05	67 109.35[a]	0.02
6	2	5	7	5	2	4	6	67 985.08[a]	−0.01	67 930.13[a]	0.03	67 169.69[a]	0.04	67 109.35[a]	0.11
6	1	5	7	5	1	4	6	67 985.08[a]	−0.02	67 930.13[a]	0.02	67 169.69[a]	0.03	67 109.35[a]	0.01
6	2	5	6	5	2	4	5	67 985.28[a]	0.01	67 930.13[a]	−0.15	67 169.69[a]	−0.14	67 109.35[a]	−0.07
6	1	5	6	5	1	4	5	67 985.28[a]	0.00	67 930.13[a]	−0.15	67 169.69[a]	−0.15	67 109.35[a]	−0.18
8	1	7	8	8	1	8	8	67 998.23[a]	0.05	67 757.60[a]	0.06				
8	2	7	8	8	0	8	8	67 998.23[a]	0.05	67 757.60[a]	0.06				
8	1	7	9	8	1	8	9	67 998.83[a]	0.05	67 758.15[a]	0.03				
8	2	7	9	8	0	8	9	67 998.83[a]	0.05	67 758.15[a]	0.03				
8	1	7	7	8	1	8	7	67 998.83[a]	−0.02	67 758.15[a]	−0.04				
8	2	7	7	8	0	8	7	67 998.83[a]	−0.02	67 758.15[a]	−0.04				
5	2	3	4	4	2	2	3	68 011.70[a]	0.08	67 923.24[a]	0.08	67 196.55[a]	0.07	67 233.88[a]	0.04
5	2	3	6	4	2	2	5	68 011.70[a]	0.00	67 923.24[a]	0.01	67 196.55[a]	0.09	67 233.88[a]	−0.04
5	2	3	5	4	2	2	4	68 011.99	0.02	67 923.51	0.0	67 196.84	0.01	67 234.20	0.00
5	3	3	4	4	2	2	3					67 197.59[a]	0.05	67 246.57[a]	0.05
5	3	3	6	4	2	2	5					67 197.59[a]	−0.02	67 246.57[a]	−0.03
5	3	3	5	4	2	2	4					67 197.91	0.02	67 246.88	0.00
3	3	1	3	2	1	2	2	68 385.63	0.00	68 215.52	0.04				
3	3	1	4	2	1	2	3	68 387.22	0.02	68 217.00	0.03				
3	3	1	2	2	1	2	1	68 387.93	0.01	68 217.73	0.07				
4	4	1	3	3	3	0	2					67 817.08[a]	0.06	68 574.65[a]	0.08
4	4	1	4	3	3	0	3					67 817.08[a]	−0.17	68 574.65[a]	−0.15
4	4	1	5	3	3	0	4					67 817.08[a]	−0.06	68 574.65[a]	−0.03
5	3	2	4	4	4	1	3							74 104.45[a]	0.09
5	3	2	6	4	4	1	5							74 104.45[a]	0.00
5	3	2	5	4	4	1	4							74 104.45[a]	−0.21

TABLE 3. (*Continued*)

J'	K_a'	K_c'	F'	J''	K_a''	K_c''	F''	$v = 0$	o.-c.	$v = 1$	o.-c.	2-^{13}C	o.-c.	3-^{13}C	o.-c.
5	4	2	4	4	4	1	3	76 412.02[a]	0.06	76 329.73[a]	0.06	75 488.65[a]	0.08	74 604.86[a]	0.06
5	4	2	6	4	4	1	5	76 412.02[a]	−0.03	76 329.73[a]	−0.02	75 488.65[a]	−0.01	74 604.86[a]	−0.03
5	4	2	5	4	4	1	4	76 412.28	−0.01	76 329.93	−0.03	75 488.65[a]	−0.23	74 605.14	0.03
4	4	0	4	3	3	1	3					75 789.78[a]	0.17		
4	4	0	3	3	3	1	2					75 789.78[a]	−0.07		
4	4	0	5	3	3	1	4					75 789.78[a]	−0.07		
8	0	8	7	7	0	7	7	77 044.64[a]	−0.02	77 019.59[a]	0.00				
8	1	8	7	7	1	7	7	77 044.64[a]	−0.02	77 019.59[a]	0.00				
8	0	8	9	7	0	7	8	77 046.44[a]	0.03	77 021.34[a]	0.06	76 122.31[a]	0.01	76 053.02[a]	0.04
8	1	8	9	7	1	7	8	77 046.44[a]	0.03	77 021.34[a]	0.06	76 122.31[a]	0.01	76 053.02[a]	0.04
8	0	8	7	7	0	7	6	77 046.44[a]	0.01	77 021.34[a]	0.04	76 122.31[a]	−0.01	76 053.02[a]	0.02
8	1	8	7	7	1	7	6	77 046.44[a]	0.01	77 021.34[a]	0.04	76 122.31[a]	−0.01	76 053.02[a]	0.02
8	0	8	8	7	0	7	7	77 046.44[a]	−0.02	77 021.34[a]	0.02	76 122.31[a]	−0.04	76 053.02[a]	−0.01
8	1	8	8	7	1	7	7	77 046.44[a]	−0.02	77 021.34[a]	0.02	76 122.31[a]	−0.04	76 053.02[a]	−0.01
7	1	6	6	6	1	5	6	77 048.09[a]	−0.04						
7	2	6	6	6	2	5	6	77 048.09[a]	−0.04						
7	1	6	6	6	1	5	5	77 049.00[a]	0.00	76 992.92[a]	0.04	76 124.89[a]	0.07	76 056.00[a]	0.01
7	2	6	6	6	2	5	5	77 049.00[a]	0.00	76 992.92[a]	0.04	76 124.89[a]	0.07	76 056.00[a]	0.01
7	1	6	7	6	1	5	6	77 049.00[a]	−0.14	76 992.92[a]	−0.10	76 124.89[a]	−0.08	76 056.00[a]	−0.13
7	2	6	7	6	2	5	6	77 049.00[a]	−0.14	76 992.92[a]	−0.10	76 124.89[a]	−0.08	76 056.00[a]	−0.13
7	1	6	8	6	1	5	7	77 049.00[a]	0.00	76 992.92[a]	0.04	76 124.89[a]	0.07	76 056.00[a]	0.01
7	2	6	8	6	2	5	7	77 049.00[a]	0.00	76 992.92[a]	0.04	76 124.89[a]	0.07	76 056.00[a]	0.01
6	3	4	5	5	3	3	4	77 052.22[a]	0.01	76 965.11[a]	0.04	76 128.10[a]	0.04		
6	3	4	7	5	3	3	6	77 052.22[a]	−0.03	76 965.11[a]	0.00	76 128.10[a]	0.00		
6	3	4	6	5	3	3	5	77 052.48	0.01	76 965.37	0.04	76 128.10[a]	−0.23		
6	2	4	5	5	2	3	4	77 053.21[a]	−0.01	76 965.97[a]	0.05	76 129.19[a]	0.09	76 071.38[a]	0.04
6	2	4	7	5	2	3	6	77 053.21[a]	−0.05	76 965.97[a]	0.01	76 129.19[a]	0.05	76 071.38[a]	0.00
6	2	4	6	5	2	3	5	77 053.49	0.00	76 966.23	0.05	76 129.19[a]	−0.18	76 071.38[a]	−0.23
9	1	8	9	9	1	9	9	77 064.61[a]	0.02						
9	2	8	9	9	0	9	9	77 064.61[a]	0.02						
9	1	8	10	9	1	9	10	77 065.19[a]	0.06						
9	2	8	10	9	0	9	10	77 065.19[a]	0.06						
9	1	8	8	9	1	9	8	77 065.19[a]	0.00						
9	2	8	8	9	0	9	8	77 065.19[a]	0.00						
4	4	0	4	3	2	1	4	77 487.71	0.05						
4	4	0	4	3	2	1	3	77 488.34	0.02	77 313.03	0.03	76 564.57[a]	0.12	77 181.59	−0.05
4	4	0	5	3	2	1	4	77 488.61[a]	0.03	77 313.27[a]	0.04	76 564.57[a]	−0.13	77 181.83[a]	−0.05
4	4	0	3	3	2	1	2	77 488.61[a]	0.02	77 313.27[a]	0.04	76 564.57[a]	−0.13	77 181.83[a]	−0.05
4	4	0	3	3	2	1	3	77 489.45	−0.03						
5	3	2	4	4	3	1	3	77 608.26[a]	0.11	77 463.68[a]	0.07	76 682.55[a]	0.04	77 061.11[a]	0.07
5	3	2	6	4	3	1	5	77 608.26[a]	0.03	77 463.68[a]	−0.01	76 682.55[a]	−0.04	77 061.11[a]	−0.01
5	3	2	5	4	3	1	4	77 608.44	0.00	77 463.95	0.05	76 682.82	0.01	77 061.46	0.13
5	4	2	4	4	3	1	3					76 779.78[a]	0.00	77 561.63[a]	0.15
5	4	2	6	4	3	1	5					76 779.78[a]	−0.09	77 561.63[a]	0.07
5	4	2	5	4	3	1	4					76 780.05	−0.04	77 561.63[a]	−0.15

[a]Blended lines: the average value was used in the fits.

At lower frequencies, separated by a range of a few tens to hundreds of MHz, lower intensity lines were observed corresponding to the first vibrationally excited state of the NH out-of-plane bending motion ($v = 1$). Since the symmetry for this state is b_1, the *ortho*/*para* statistical weights associated with K_a parity are reversed compared to the ground state (*ortho* for odd K_a, *para* for even K_a). Consequently, the Boltzmann population ratio at room temperature ($N_1/N_0 \simeq 1/10$) results in relative intensity ratios I_1/I_0 of ~1/6 for transitions originating from odd K_a levels and 1/16.7 for those from even K_a levels. This effect is illustrated in

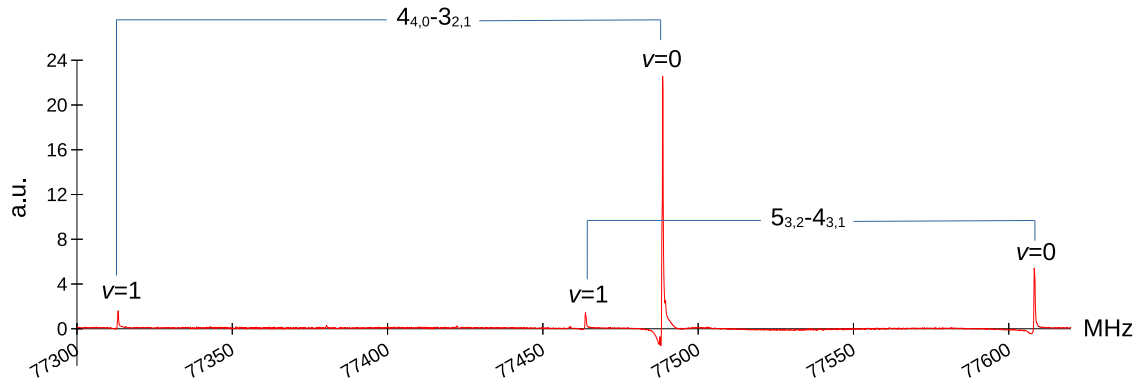

FIG. 2. Rotational spectrum recorded in the 77 300–77 620 MHz frequency region using a FJ-AMMW spectrometer. The $4_{4,0}$–$3_{2,1}$ and $5_{3,2}$–$4_{3,1}$ rotational transition lines for both the ground state ($v = 0$) and the first vibrationally excited state of the NH out-of-plane bending ($v = 1$) are shown. The relative intensity of the lines reflects the opposite statistical weight of the rotational levels with different K_a parity in the ground and vibrationally excited states.

Fig. 2, which provides an excerpt of the recorded spectrum comparing the $4_{4,0}$–$3_{2,1}$ and $5_{3,2}$–$4_{3,1}$ transition lines, and the observed relative intensities across the spectrum are consistent with these expectations.

The pure rotational transition lines of both the ground and the first excited states measured in this work were included in a global fit, alongside with the pure rotational transition lines of the ground state listed in the literature[4,5,7,8] and the 16_0^1, 16_0^2 and 16_1^2 vibro-rotational transition lines measured by Tokaryk and van Wijngaarden[15] and retrieved from the supplementary material of the same article. We also accounted for the measurements of Hegelund, Larsen, and Palmer[14] on the 16_0^2 band, which, despite the lower accuracy, span a larger frequency range. For transition lines reported in more than one dataset, the values with better accuracy were chosen.

Ray's asymmetry parameter $\kappa = (2B - A - C)/(A - C)$[24] is 0.9438, classifying pyrrole as a near-symmetric oblate rotor. Therefore, the *S*-reduction in the III^{ℓ}-representation was selected for the fit. The lines were assigned using the CALPGM program suite[25] through direct diagonalization of the following Hamiltonian:

$$H = H_0 + H_1 + H_2 + \Delta E_0^1 + \Delta E_0^2 \tag{2}$$

where the H_v terms represent the Hamiltonian of the $v = 0, 1, 2$ vibrational states and ΔE_0^v are the energy differences between the ground state and the first and second vibrational excited states of the NH out-of-plane bending mode. Specifically:

$$\begin{aligned} H_0 &= H_{0,ROT} + H_{0,CD} + H_{0,NQC} \\ H_1 &= H_{1,ROT} + H_{1,CD} + H_{1,NQC} \\ H_2 &= H_{2,ROT} + H_{2,CD} \end{aligned} \tag{3}$$

where H_{ROT} represents the rigid rotor related to the *A*, *B*, and *C* rotational constants, H_{CD} accounts for the centrifugal distortion effect and H_{NQC} is the operator associated with the coupling of the ^{14}N nuclear spin ($I = 1$) with the overall rotation, leading to the hyperfine structure of the rotational transition lines. The uncertainties applied to each set of pure rotational lines are given in Table 1. For the vibrorotational transitions, uncertainties of 0.0001 and 0.0010 cm^{-1} were used for the datasets of Tokaryk and van Wijngaarden[15] and Hegelund, Larsen, and Palmer,[14] respectively. In the global fitting procedure, unblended lines were assigned a weight of unity. For blended lines, a weight of $1/n$ was applied, where n denotes the number of transitions contributing to the observed frequency; this accounts for the reduced certainty in their individual assignments. The resulting spectroscopic parameters, summarised in Table 4, successfully reproduce the newly observed rotational transition frequencies to within the instrumental accuracy of 0.05 MHz. Instances in Table 3 where residuals (observed minus calculated) surpass this accuracy are characteristic of these blended lines, for which their average frequency was utilised in the fit.

In order to compare our results with previous ones, we also performed the fit applying the I^r-representation in the *S*-reduction and report the determined parameters in the same table with the data from the literature. The input and output fitting files related to the SPFIT program of the CALPGM suite[25] can be found in the AMS Acta repository in text format for both the III^{ℓ} and I^r representations.[26] The input and output prediction files related to the SPCAT program are provided as well.

4.2. ^{13}C isotopologues

The natural abundance of the carbon-13 isotope is ~1%. Due to molecular symmetry, the two carbon atoms alpha (α) to the amine group (C2 and C5 in Fig. 1) are equivalent, as are the two carbon atoms located in the β position (C3 and C4 in Fig. 1). Consequently, two ^{13}C-isotopologues exist with an abundance of about 2%. With respect to the normal species, isotopic substitution reduces the symmetry of the system to C_s, eliminating the statistical nuclear spin-weight effect. Regarding the principal axis system (PAS), the orientation of the *a* and *b* axes changes while *c* remains perpendicular to the planar ring, as depicted in Fig. 3. As a result, the μ_a electric dipole moment component decreases in favor of the μ_b component, allowing both *a*- and *b*-type lines to be observed in the pure rotational spectra.

TABLE 4. Experimental spectroscopic parameters (*S*-reduction) of pyrrole obtained from the simultaneous fit of the pure rotation and vibration–rotation transition lines of the ground state ($v = 0$), first ($v = 1$) and second ($v = 2$) vibrational excited NH out-of-plane bending states. Literature data are converted using $c = 2.997\,924\,58 \times 10^{10}$ cm s^{-1} as conversion factor. The standard deviations are indicated in parentheses in the unit of the last quoted digit

III^{ℓ}-representation	$v = 0$	$v = 1$	$v = 2$
ΔE_0^v (THz)	0	14.229 575 62(16)	28.861 646 08(14)
A (MHz)	9130.633 69(37)	9110.345 41(98)	9095.270 38(96)
B (MHz)	9001.363 55(36)	8988.315 42(96)	8978.562 74(100)
C (MHz)	4532.109 94(37)	4531.542 15(96)	4530.008 28(69)
D_J (kHz)	2.926 58(31)	2.923 68(37)	2.912 63(36)
D_{JK} (kHz)	−4.649 54(79)	−4.6322(21)	−4.6332(13)
D_K (kHz)	2.0264(11)	2.0085(25)	2.0313(15)
d_1 (kHz)	0.061 61(48)	0.061 21(55)	0.058 63(56)
d_2 (kHz)	0.022 24(41)	0.021 87(41)	0.024 49(41)
H_{JK} (mHz)	−4.90(28)	−4.8 (11)	−5.60(40)
H_{KJ} (mHz)	5.76(39)	3.6 (13)	6.66(48)
$1.5 \cdot \chi_{cc}$ (MHz)	−4.0499(70)	−3.904(54)	⋯
$0.25 \cdot (\chi_{bb}\text{-}\chi_{aa})$ (MHz)	−0.0293(20)	⋯	⋯
N_{mw};[4] σ (MHz)	39; 0.092	⋯	⋯
N_{mw};[5] σ (MHz)	19; 0.007	⋯	⋯
N_{mw};[7] σ (MHz)	30; 0.003	⋯	⋯
N_{mmw}; σ (MHz)	39; 0.024	33; 0.035	⋯
N_{mmw};[8] σ (MHz)	92; 0.034	⋯	⋯
N_{IR};[14] σ (cm^{-1})	⋯	⋯	1177; 0.000 72 16_0^2
N_{IR};[15] σ (cm^{-1})	2252; 0.000 13 16_0^1	1438; 0.000 12 16_1^2	1699; 0.000 19 16_0^2
I^r-representation	$v = 0$	$v = 1$	$v = 2$
ΔE_0^v (THz)	0	14.229 575 52(17)	28.861 645 49(16)
A (MHz)	9130.634 98(44)	9110.347 74(145)	9095.282 72(162)
B (MHz)	9001.362 70(39)	8988.314 23(108)	8978.560 49(106)
C (MHz)	4532.110 79(38)	4531.545 14(69)	4530.008 47(56)
D_J (kHz)	1.009 39(65)	1.012 53(75)	1.000 55(75)
D_{JK} (kHz)	2.7949(56)	2.7837(64)	2.8284(58)
D_K (kHz)	−0.7887(68)	−0.7827(80)	−0.8217(70)
d_1 (kHz)	−0.614 24(11)	−0.613 50(20)	−0.609 32(20)
d_2 (kHz)	−0.260 66(29)	−0.259 04(29)	−0.263 12(30)
H_{JK} (mHz)	−6.24(99)	−6.0(20)	−7.6(11)
H_{KJ} (mHz)	11.11(91)	11.0(25)	17.6(12)
$1.5 \cdot \chi_{aa}$ (MHz)	2.1135(64)	1.92(11)	⋯
$0.25 \cdot (\chi_{bb}\text{-}\chi_{cc})$ (MHz)	0.9984(21)	0.989(21)	⋯
I^r-representation (literature)	$v = 0$[13]	$v = 1$[15]	$v = 2$[15]
ΔE_0^v (THz)	0	14.229 575 04(26)	28.861 645 72(25)
A (MHz)	9130.632 14(30)	9110.343 45(156)	9095.269 17(138)
B (MHz)	9001.362 84(66)	8988.320 58(159)	8978.566 68(153)
C (MHz)	4532.110 92(63)	4531.549 25(10)	4530.011 30(138)
D_J (kHz)	1.008 98(96)	1.014 71(69)	1.000 89(78)
D_{JK} (kHz)	2.7926(69)	2.8046(33)	2.8570(39)
D_K (kHz)	−0.7936(87)	−0.8206(28)	−0.8808(33)
d_1 (kHz)	−0.614 19(20)	−0.613 74(30)	−0.609 54(39)
d_2 (kHz)	−0.261 36(39)	−0.259 87(15)	−0.264 87(21)
H_{JK} (mHz)	−14.3(10)	⋯	⋯
H_{KJ} (mHz)	17.4(10)	⋯	⋯

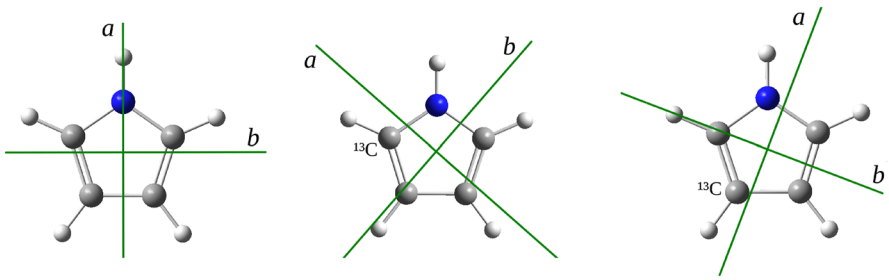

FIG. 3. Orientation of the principal inertial axes in the normal species and the two ^{13}C-isotopologues of pyrrole.

In agreement with the above considerations, we detected several μ_a and μ_b-type rotational transition lines of the ^{13}C-isotopologues in natural abundance, and some of them showed a resolved nuclear hyperfine structure. The newly measured lines are listed in Table 3. These lines were included in a global fit along with the lines reported by Nygaard *et al.*[4] using the Hamiltonian H_0 as described in Eq. (3). Since the nuclear quadrupole coupling constant χ_{cc} is expected to remain unchanged upon isotopic substitution (the molecule remains planar), its value was fixed to that of the normal species. Due to insufficient data to determine it precisely, the $\chi_{bb}-\chi_{aa}$ term could not be fitted and was therefore kept fixed at zero. The achieved spectroscopic constants are listed in Table 5. The fitting and prediction files related to the SPFIT and SPCAT programs of the CALPGM suite[25] can be found in the AMS Acta repository in text format.[26]

TABLE 5. Experimental spectroscopic parameters (S-reduction) of the ^{13}C isotopologues of pyrrole. The value of χ_{cc} is fixed to that of the normal species. The weighted standard deviations are indicated in parentheses in the unit of the last quoted digit

III^{ℓ}-representation	2-^{13}C	3-^{13}C
A (MHz)	9021.8767(54)	9099.1275(55)
B (MHz)	8892.7296(54)	8803.1373(57)
C (MHz)	4477.7409(72)	4473.6768(70)
D_J (kHz)	3.07(11)	3.13(12)
D_{JK} (kHz)	−4.716(46)	−4.729(77)
D_K (kHz)	1.854(99)	1.93(11)
d_1 (kHz)	...	0.063(19)
d_2 (kHz)	−0.018 84(23)	...
$1.5\cdot\chi_{cc}$ (MHz)	(−4.05)	(−4.05)
N_{mw};[4] σ (MHz)	39; 0.084	23; 0.082
N_{mmw}; σ (MHz)	24; 0.038	28; 0.040

The ratios between the μ_a and μ_b electric dipole moment components of 2-^{13}C and 3-^{13}C isotopologues were estimated from relative intensity measurements of three pairs of R-type transitions involving the same initial level: (i) $5_{2,3}$–$4_{3,2}$ and $5_{3,3}$–$4_{3,2}$, shown in Fig. 4; (ii) $5_{2,3}$–$4_{2,2}$ and $5_{3,3}$–$4_{2,2}$; (iii) $5_{3,2}$–$4_{3,1}$ and $5_{4,2}$–$4_{3,1}$, see Table 3 for the frequencies. Specifically, it was found that μ_a^2:μ_b^2 = 4:10 for the 2-^{13}C species and μ_a^2:μ_b^2 = 40:10 for the 3-^{13}C species. Since the total electric dipole moment does not change upon isotopic substitution but the principal axis system rotates, the rotation angle ϑ can be derived using the relationship $\tan\vartheta = \mu_b/\mu_a$ The determined values are compared in Table 6 to those derived by Nygaard *et al.*[4] using an inertial approach. The rotation angle derived from intensities for the 2-^{13}C species ($\vartheta = 57.7°$) agrees well ($\Delta\vartheta = 0.4°$) with the value derived from the inertial analysis by Nygaard *et al.*[4] ($\vartheta = 57.3°$). However, for the 3-^{13}C species, the angle derived from intensities ($\vartheta = 26.6°$) shows a larger difference ($\Delta\vartheta = 2.8°$) compared to the inertial analysis value (23.8°). These differences can be explained by the error associated with the estimation of the experimental μ_a^2:μ_b^2 ratios. Using these sets of angle values and the experimental value

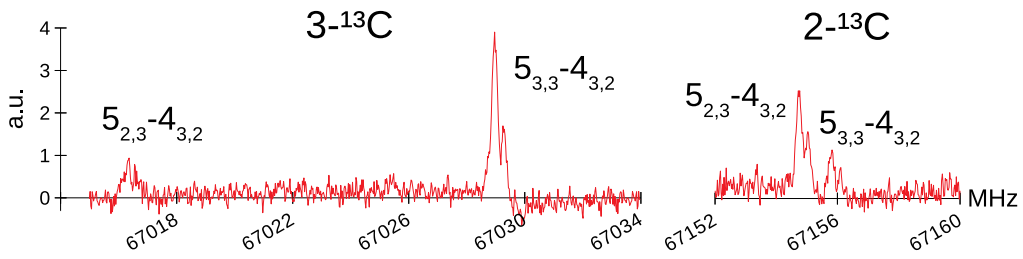

FIG. 4. Rotational spectrum recorded in the 67 015–67 034 and 67 152–67 160 MHz frequency regions using a FJ-AMMW spectrometer. The μ_a-type $5_{3,4}$–$4_{3,2}$ and μ_b-type $5_{2,3}$–$4_{3,2}$ rotational transition lines for both the 2-^{13}C and 3-^{13}C isotopologues are shown. The intensity of the lines is proportional to the $|\mu_a|^2$ and $|\mu_b|^2$ values in the corresponding isotopologues.

TABLE 6. Rotation angle of the *ab* inertial plane of the ^{13}C isotopologues with respect to the normal species and derived electric dipole moment components

2-^{13}C	ϑ/°	$\lvert\mu_a\rvert$ (D)	$\lvert\mu_b\rvert$ (D)
Relative intensity	57.7	0.944	1.494
Isotopic substitution	57.3[4]	0.955	1.487
3-^{13}C	ϑ/°	$\lvert\mu_a\rvert$ (D)	$\lvert\mu_b\rvert$ (D)
Relative intensity	26.6	1.580	0.791
Isotopic substitution	23.8[4]	1.617	0.713

μ_{tot} = 1.767(2) D,[7] the components of the electric dipole moment reported in Table 6 were obtained.

5. Discussion

In this work, we report newly measured pure rotational lines for both the ground state and the first vibrationally excited state of pyrrole. Although observing excited states is uncommon in supersonic expansion, it is not unprecedented. For instance, using the same spectrometer, we observed the spectra of five vibrational states of pyridine between 370 and 700 cm^{-1}.[27] We propose a global fit that includes 252 pure rotational spectral lines and 6566 rovibrational spectral lines involving the NH out-of-plane bending states, based on the III^{ℓ} representation in the *S*-reduction. This choice, suitable for a planar, near-oblate rotor like pyrrole, has the advantage of minimizing the contribution of the in-plane χ_{bb}–χ_{aa} nuclear quadrupole constant in favor of the χ_{cc} out-of-plane component. This approach facilitates fitting when limited information is available. For example, in the case of v = 1 using the III^{ℓ}-representation it is reasonable to set χ_{bb}–χ_{aa} = 0 and this choice allows determining χ_{cc} with a relative error of 1.4%. Conversely, using the I^r-representation, both χ_{bb}–χ_{cc} = 0 and χ_{aa} constants must be fitted, resulting in increased uncertainty (5.7% and 2.1%, respectively). Similarly, for the ^{13}C isotopologues, where the perpendicular component can be considered unchanged upon substitution, using the III^{ℓ} representation allows reproduction of the experimental data by fixing this constant to the value of the normal species and neglecting the planar component. The consistency of the fitted parameters across the different vibrational states and isotopologues, along with standard deviations consistent with experimental uncertainties for each dataset, demonstrates the robustness and overall reliability of the global model presented and the derived reference parameters. Two sextic centrifugal distortion constants (H_{JK} and H_{KJ}) were determined for all three vibrational states (v = 0, 1, 2) of the normal species. Although associated with relatively large uncertainties, particularly for v = 1 and v = 2, their signs and orders of magnitude appear reliable and consistent across the states.

Comparison with previous data can be done considering the I^r-representation. The corresponding parameters are also given in Table 4 with those reported by Tokaryk and van Wijngaarden.[15] The values are similar, but not identical within the error. The main differences arise primarily because our fit incorporates ^{14}N hyperfine structure for v = 0 and v = 1 and includes sextic centrifugal distortion constants (H_{JK} and H_{KJ}) for v = 1 and v = 2, which were not part of the earlier analysis. This leads to statistically significant differences, notably in the values of H_{JK} and H_{KJ} in the ground state.

TABLE 7. Fundamental and first overtone wavenumbers for the NH out-of-plane bending of pyrrole (ν_{16}). The standard deviations are indicated in parentheses in the unit of the last quoted digit

	16_0^1	16_0^2
III^{ℓ}	474.647 552(5)	962.720 890(5)
I^r	474.647 548(6)	962.720 865(6)
I^r[15]	474.647 539 2(88)	962.720 874 1(85)

TABLE 8. Nuclear quadrupole coupling constants for pyrrole. The standard deviations are indicated in parentheses in the unit of the last quoted digit

	v = 0	v = 0[6]	v = 1
χ_{aa} (MHz)	1.409(6)	1.405 53(3)	
χ_{bb} (MHz)	1.291(6)	1.264 11(6)	
χ_{cc} (MHz)	−2.700(5)	−2.669 64(9)	−2.60(4)

For convenience, the fundamental and first overtone wavenumbers for the NH out-of-plane bending obtained with the two representations and the literature data[15] are summarized in Table 7.

Regarding the nuclear quadrupole coupling constants (Table 8), our results differ from the high-resolution values obtained by Gaines *et al.*[6] using maser spectroscopy. Unfortunately, the data used in 1974 are only partially available and in graphical form, making it impossible to include them in a new model. It is worth noting that, because of the change in the vibrational wavefunction and electric field gradient upon excitation of the out-of-plane NH bending mode, the absolute value of χ_{cc} decreases in going from the ground state [χ_{cc} = −2.700(5) MHz] to the first excited state [χ_{cc} = −2.60(4) MHz].

6. Conclusions

This work presents new high-resolution measurements of pyrrole in the 59.6–78.3 GHz range using a free-jet millimeter-wave Stark-modulated absorption spectrometer We have successfully assigned and analyzed the rotational spectra for the normal isotopologue in its vibrational ground state and the first excited state of the NH out-of-plane bending mode, as well as for the two distinct ^{13}C monosubstituted isotopologues in natural abundance. The ^{14}N nuclear quadrupole hyperfine structure was resolved and included in the analysis for all observed species.

A comprehensive global fit was performed, incorporating our new rotational data with previously published microwave, millimeter-wave, and high-resolution infrared data pertaining to the NH out-of-plane bending mode (fundamental 16_0^1, first overtone 16_0^2, and first hot band 16_1^2). Using Watson's S-reduction in the III^{ℓ} representation, which is well-suited for this near-oblate rotor, we derived a refined and self-consistent set of spectroscopic parameters. This set includes rotational constants, quartic and sextic centrifugal distortion constants for the v = 0, 1, and 2 states for the normal

species and nuclear quadrupole coupling constants for the $v = 0$ and 1 states. Updated rotational global fits are also provided for the ^{13}C isotopologues.

The resulting parameters provide an improved description of the ground and low-lying vibrational states of pyrrole, demonstrating good consistency across the different datasets and reproducing the experimental transition frequencies within their uncertainties. These precise rotational and rovibrational data significantly enhance the spectroscopic database for pyrrole, a fundamental heterocyclic molecule and a key structural unit in vital biomolecules. The refined parameters will be valuable for astrophysical searches and for benchmarking theoretical calculations. While the overall model is robust, minor discrepancies with some previous determinations, particularly regarding higher-order centrifugal distortion terms and nuclear quadrupole constants, highlight areas where further investigation could be beneficial. The presented line list and parameters are made available to support future studies.

Acknowledgments

We are grateful to Professor René Wugt Larsen for providing the list of the 16_0^2 band transition lines. We acknowledge the support of the author community in using REVTEX. We acknowledge the CINECA award under the ISCRA initiative, for the availability of high-performance computing resources and support. A. M. thanks the University of Bologna for financial support (RFO, Ricerca Fondamentale Orientata). LE and SM acknowledge the project PRIN2022 (MUR code 2022WKTH9E and CUP J53D23008810006) funded by the European Union - Next Generation EU. This research is a contribution to the Italian Space Agency (project HELENA, Award Nos. 2023-9-U.0 and CUP-F33C23000310006) and the Emilia-Romagna Region (POR FESR 21-27, project SMAL-SAT, Award Nos. PG/2023/308391 and CUP-J47G22000720003).

7. Author Declarations

7.1. Conflict of interest

The authors have no conflicts to disclose.

8. Data Availability

The data that support the findings of this study are openly available in University of Bologna repository, at https://doi.org/10.6092/unibo/amsacta/8327.

9. References

[1] S. Fox and H. Strasdeit, Astrobiology **13**, 578 (2013).
[2] W. S. Wilcox and J. H. Goldstein, J. Chem. Phys. **20**, 1656 (1952).
[3] B. Bak, D. Christensen, L. Hansen, and J. Rastrup-Andersen, J. Chem. Phys. **24**, 720 (1956).
[4] U. Nygaard, J. T. Nielsen, J. Kirchheiner, G. Maltesen, J. Rastrup-Andersen, and G. O. Sørensen, J. Mol. Struct. **3**, 491 (1969).
[5] K. Bolton and R. Brown, Aust. J. Phys. **27**, 143 (1974).
[6] L. Gaines, P. Thaddeus, G. Tomasevich, and K. Tucker, NASA Technical Report, 1974, Vol. **79**.
[7] R. K. Bohn, K. W. Hillig, II, and R. L. Kuczkowski, J. Phys. Chem. **93**, 3456 (1989).
[8] G. Wlodarczak, L. Martinache, J. Demaison, and B. P. Van Eijck, J. Mol. Spectrosc. **127**, 200 (1988).
[9] C. P. Endres, S. Schlemmer, P. Schilke, J. Stutzki, and H. S. P. Müller, J. Mol. Spectrosc. **327**, 95 (2016).
[10] J. K. Eloranta, Z. Naturforsch. A **25**, 1296 (1970).
[11] A. Mellouki, R. Georges, M. Herman, D. L. Snavely, and S. Leytner, Chem. Phys. **220**, 311 (1997).
[12] A. Held and M. Herman, Chem. Phys. **190**, 407 (1995).
[13] A. Mellouki, J. Vander Auwera, and M. Herman, J. Mol. Spectrosc. **193**, 195 (1999).
[14] F. Hegelund, R. W. Larsen, and M. Palmer, J. Mol. Spectrosc. **252**, 93 (2008).
[15] D. W. Tokaryk and J. A. van Wijngaarden, Can. J. Phys. **87**, 443 (2009).
[16] H. Zarringhalam, "High-resolution laser and far-infrared Fourier transform synchrotron-based spectroscopy of selected molecules," Ph.D. thesis, University of New Brunswick, 2022.
[17] M. Carlotti, G. Di Lonardo, G. Galloni, and A. Trombetti, J. Chem. Soc., Faraday Trans. **2**(68), 1473 (1972).
[18] C. Calabrese, A. Maris, L. Evangelisti, L. B. Favero, S. Melandri, and W. Caminati, J. Phys. Chem. A **117**, 13712 (2013).
[19] C. Calabrese, A. Vigorito, A. Maris, S. Mariotti, P. Fathi, W. D. Geppert, and S. Melandri, J. Phys. Chem. A **119**, 11674 (2015).
[20] A. Vigorito, C. Calabrese, S. Melandri, A. Caracciolo, S. Mariotti, A. Giannetti, M. Massardi, and A. Maris, Astron. Astrophys. **619**, A140 (2018).
[21] F. Sun, A. Maris, L. Evangelisti, W. Song, S. Melandri, J. R. Morán, C. Calabrese, and A. Lesarri, J. Phys. Chem. A **129**, 109 (2025).
[22] A. Mellouki, J. Liévin, and M. Herman, Chem. Phys. **271**, 239 (2001).
[23] W. Gordy and R. Cook, *Microwave Molecular Spectra* (Wiley, New York, NY, 1984).
[24] B. S. Ray, Z. Phys. **78**, 74 (1932).
[25] H. M. Pickett, J. Mol. Spectrosc. **148**, 371 (1991).
[26] A. Maris (2024). "Reference data for isolated pyrrole," University of Bologna, Bologna. https://doi.org/10.6092/unibo/amsacta/8327
[27] A. Maris, L. B. Favero, R. Danieli, P. G. Favero, and W. Caminati, J. Chem. Phys. **113**, 8567 (2000).
[28] P. R. Bunker and P. Jensen, *Molecular Symmetry and Spectroscopy*, 2nd ed. (NRC Research Press, Ottawa, 1998).
[29] R. S. Mulliken, J. Chem. Phys. **23**, 1997 (1955).